c-1

NACA

RESEARCH MEMORANDUM

AN EXPERIMENTAL INVESTIGATION OF TWO METHODS FOR REDUCING TRANSONIC DRAG OF SWEPT-WING AND BODY COMBINATIONS

By John B. McDevitt

Ames Aeronautical Laboratory
Moffett Field, Calif.

NATIONAL ADVISORY COMMITTEE
FOR AERONAUTICS

WASHINGTON
April 29, 1955

NATIONAL ADVISORY COMMITTEE FOR AERONAUTICS

RESEARCH MEMORANDUM

AN EXPERIMENTAL INVESTIGATION OF TWO METHODS FOR REDUCING TRANSONIC DRAG OF SWEPT-WING AND BODY COMBINATIONS

By John B. McDevitt

SUMMARY

A wing swept back 35°, in combination with one basic body and three modified bodies, was investigated at Mach numbers from 0.60 to 1.20. The tests, which included measurements of forces and pressure distributions, were conducted in the Ames 2- by 2-foot transonic wind tunnel. The wing had an aspect ratio of 6, a taper ratio of 0.5, and NACA 64_2A015 sections normal to the mid-chord line which was swept back 35°. The basic body was a Sears-Haack body having a fineness ratio of 9. One of the modified bodies was indented according to the area rule so as to reduce the wave drag at a Mach number of 1. The other two modified bodies were designed by the ring-vortex method of Kuchemann for alleviating all, or part of, the adverse interference at the root of the sweptback wing in an attempt to obtain the full benefit of sweep for delaying the drag rise. Both methods resulted in considerable reductions in drag at transonic speeds.

INTRODUCTION

It is well known that the full benefit of sweepback for reducing compressibility drag at high subsonic Mach numbers is generally not realized in practice largely because of losses near the wing root and near the wing tips. Because of reflection at the plane of symmetry the velocity field near the root of the sweptback wing at subsonic speeds is distorted from that for the infinite wing (refs. 1 and 2). The velocity distortion can be corrected to some extent either by altering the wing geometry or by contouring the body in the vicinity of the wing. Shaping the body to conform to the streamlines of the oblique wing has been suggested in reference 3 (see also refs. 4 and 5). The use of ring vortices for determining the body shape has been studied in considerable detail by Kuchemann and Weber (refs. 6 and 7). Recent experimental investigations (refs. 8 to 10) of the ring-vortex method of Kuchemann have shown that considerable reductions in drag at high subsonic Mach numbers can be obtained by use of this method.

It is realized, of course, that the Kuchemann method cannot be realistically applied at a design Mach number too close to 1 because of the general inadequacy of linearized subsonic flow theory which is used. Near a Mach number of 1, a general rule concerning wave drag (that wave drag depends only on the axial distribution of cross-sectional area) has been demonstrated in a convincing manner by Whitcomb (ref. 11), at least for configurations of sufficient slenderness. However, this area rule cannot be expected to provide the ultimate design procedure when the combination of wing aspect ratio and thickness-to-chord ratio is large.

The purpose of the present investigation is to extend the previous experimental investigations of the Kuchemann method to transonic Mach numbers and to compare the results with those obtained by application of Whitcomb's area rule.[1] The present report gives the results of an experimental investigation at Mach numbers from 0.60 to 1.20 of one basic (Sears-Haack) body and three modified bodies in combination with a wing swept back 35°. One of the modified bodies was shaped by application of the ring-vortex method of Kuchemann so as to cancel the distortion velocity in the chord plane at the juncture of the fuselage and the sweptback wing.

The distortion velocity was assumed to be equal to the sum of the unmodified-body disturbance velocity and the distortion velocity at the center line of the sweptback wing. Another of the modified bodies was shaped in a manner roughly similar to the Kuchemann modification but the maximum change in body radius was approximately one half that for the Kuchemann modification. This model was tested in order that some indication of the effects of a reduced amount of body modification could be obtained. The third model was indented according to the area rule in such a way that the axial distribution of cross-sectional area was equivalent to that of a Sears-Haack body.

It should be kept in mind that the area-rule and Kuchemann modifications are based on entirely different concepts. Kuchemann's method uses ring vortices to shape the body so as to follow the streamline of the oblique wing but does not necessarily involve a change in body volume, whereas the area rule removes from the body the entire exposed volume of the wing. Furthermore, it should be recognized that the area rule is general in its application while Kuchemann's method is restricted to swept-wing and body combinations.

---

[1]A similar experimental study by Howell and Braslow (ref. 12) has been published recently. The results presented in reference 12 indicate that the two concepts can be combined to give greater drag reduction than can be obtained by either concept alone.

NOTATION

A	aspect ratio
b	wing span
C_D	drag coefficient, $\frac{\text{drag}}{qS}$
C_L	lift coefficient, $\frac{\text{lift}}{qS}$
C_m	pitching-moment coefficient, $\frac{\text{pitching moment about } \bar{c}/4}{qS\bar{c}}$
C_p	pressure coefficient, $\frac{\text{(local static pressure)} - \text{(free-stream static pressure)}}{q}$
c	local wing chord
$\bar{c}$	wing mean aerodynamic chord, $\frac{\int_0^{b/2} c^2 dy}{\int_0^{b/2} c\, dy}$
c_j	chord at wing-body junction (chord through the point of intersection of basic body and mid-chord line of the swept wing)
l	body length (distance from nose to theoretical point of closure)
M	free-stream Mach number
M_{cr}	wing critical Mach number based on simple-sweep concepts
M_{des}	design Mach number
q	free-stream dynamic pressure, $\frac{1}{2}\rho V_o^2$
r	body radius
r_o	maximum body radius
r_j	radius of basic body at intersection with mid-chord line of swept wing

S	wing area
u	streamwise perturbation velocity
V_o	free-stream velocity
x	distance behind body nose
α	angle of attack
λ	wing taper ratio
Λ	angle of sweep, positive when swept back
ξ	distance behind wing leading edge, dimensionless with respect to wing chord
ξ_j	distance behind the leading edge of the wing-body junction, dimensionless with respect to the wing chord at the wing-body junction
ρ	free-stream density

APPARATUS AND MODELS

Apparatus

The tests were conducted in the Ames 2- by 2-foot transonic wind tunnel which is of the variable-density type and is equipped with a perforated test section which permits testing models at any speed from the subsonic to the low supersonic.

The models were mounted on a sting as shown in figure 1. The normal and chord forces and the pitching moment were measured with electrical strain gages enclosed within the model. Multiple-tube mercury manometers, connected to pressure orifices in the model by flexible tubing, were photographed to provide records of the pressure distributions on the models. The force and pressure-distribution tests were made separately.

Models

Plan forms of the four wing-body combinations are shown in figure 2. The wing used in combination with the various bodies had an aspect ratio of 6, a taper ratio of 0.5, and NACA 64_2A015 sections normal to the 50-percent-chord line which was swept back 35°. The center lines of the

bodies were located in the chord plane of the wing and all bodies were truncated, as shown in figure 2, to permit mounting on the sting. All the bodies, basic and modified, had circular cross sections.

Basic model.- The wing-body combination designated basic model, see figure 2(a), had a body of revolution shaped according to the Sears-Haack formula

$$\frac{r}{r_o} = \left[1 - \left(1 - \frac{x}{l/2}\right)^2\right]^{3/4}$$

The body fineness ratio was 9 based on the theoretical length of body to closure and the maximum body diameter.

Models 1 and 2.- Plan forms of models 1 and 2 are shown in figures 2(b) and 2(c). Before modification, both models were identical to the basic model described above. Further details concerning the body shapes in the vicinity of the wing-body junction are given in figure 3.

The body for model 1 was shaped arbitrarily and had approximately one half the maximum radial modification of model 2. (See fig. 3.) This modification reduced the basic body volume by about 2 percent.

The body shape for model 2 (referred to in the following discussion of the experimental data as the Kuchemann modification) was calculated by the ring-vortex method of references 6 and 7. Further details concerning the ring-vortex method, as used here, are to be found in the appendix of reference 8.[2] The body was shaped (design Mach number 0.87) so as to induce at the junction a perturbation velocity of sufficient strength to cancel the sum of the basic body velocity and the distortion velocity at the center line of the sweptback wing. No special attempt was made to cancel disturbances upstream or downstream of the junction. Calculated values of the perturbation velocities induced by the Kuchemann body modification are shown in figure 4. This modification reduced the basic body volume by about 5 percent.

Area-rule model.- The wing-body combination designated as the area-rule model was designed by consideration of Whitcomb's rule for the reduction of wave drag at a Mach number of 1. The body was indented so that the axial distribution of cross-sectional area for the wing-body combination was equivalent to that of a Sears-Haack body having a fineness ratio of 9. Since the exposed volume of the wing was substantial (approximately 24 percent of the basic body volume) it seemed reasonable

[2]The additional modification (leading to elliptical, instead of circular, body cross sections) described in the appendix of reference 8 has not been applied in the present case.

to increase the body size for this model so that the indented body had an enclosed volume equal to that enclosed by the original basic body. Details of the body shape near the wing-body junction are presented in figure 3.

Axial distributions of cross-sectional areas.- The axial distributions of cross-sectional areas for the various bodies and the various wing-body combinations are shown in figure 5.

Location of pressure orifices.- The spanwise location of the wing pressure orifices is shown in figure 2. Nine orifices were along the wing upper surface, starting at 5-percent chord and terminating at 85-percent chord, and eight orifices were along the wing lower surface, starting at 10-percent chord and terminating at 80-percent chord.

A single row of 16 pressure orifices, starting at the leading edge of the wing-body junction line and spaced 0.343 inch apart, was located at one side of the body. The first 10 or 11 orifices were as close as feasible to the body intersection line of the upper surface of the wing; the remaining orifices were in the wing chord plane downstream of the wing trailing edge.

TESTS AND PROCEDURE

The models were tested through the Mach number range from 0.60 to 1.20 with the tunnel operating at atmospheric total pressure. The corresponding Reynolds number (based on wing mean aerodynamic chord) varied from approximately 0.8×10^6 to 1.0×10^6 (fig. 6). For most of the Mach number range the angle of attack was limited because of stress limits on the balance flexures.

Tunnel-boundary-interference corrections were not applied to the data. These effects at subsonic speeds were known to have been minimized by the perforated test section. In the Ames 2- by 2-foot transonic wind tunnel, for models of the size employed in the present investigation, the influence of the reflected waves on model characteristics is small and confined to the Mach number range from 1.00 to about 1.15. The magnitude of the effects of the reflected waves is not considered sufficiently great to affect the conclusions given in this report.

The drag data have been corrected for an interaction in the balance mechanism of normal force on chord force and have been adjusted to represent free-stream static pressure at the model base. Corrections have been applied to the angle-of-attack settings to account for sting deflection under aerodynamic loading of the model.

RESULTS

Force Studies

The drag, lift, and pitching-moment coefficients of the four models are presented in figure 7. Cross plots, which summarize the more important of the drag and lift characteristics, are presented in figures 8 and 9.

Drag.- The variation of zero-lift drag coefficient with Mach number is shown in figure 8(a). The lowest drag at the high subsonic Mach numbers was obtained by the area-rule modification, the drag rise of this model being virtually eliminated up to 0.9 Mach number. On the other hand, at supersonic speeds the Kuchemann modification (model 2) resulted in the lowest drag. It is significant to note the substantial reduction of wave drag obtained by the body modification of model 1, in view of the fact that this particular model was modified a comparatively slight amount.

The variation of drag coefficient at $0.3C_L$ with Mach number is shown in figure 8(b). The reductions in drag obtained by the various modifications are comparable to the drag reductions at zero lift. The drag coefficients for the area-rule model and the Kuchemann model are in close agreement throughout most of the high subsonic Mach number range but the Kuchemann model had considerably lower drag at supersonic Mach numbers.

Lift.- The variation of lift-curve slope (evaluated at zero lift) with Mach number is shown in figure 9. The four models had approximately the same values of lift-curve slope at subcritical speeds[3] but significant differences occurred at transonic Mach numbers. As might be expected, the basic model had the lowest lift-curve slopes at high subsonic speeds. However, the basic model had the highest lift-curve slopes for Mach numbers above about 1.13.

Modifying the body shapes improved the lift characteristics considerably at high subsonic Mach numbers where not only higher values but also smoother variations of lift-curve slope with increasing Mach number were obtained. Near a Mach number of 1.0 the highest lift-curve slopes were obtained as a result of the Kuchemann modification.

Moment.- An attempt to analyze the pitching-moment data has not been made since it is well known that moment data for swept wings are particularly sensitive to Reynolds number and attempts to use these data for full-scale configurations would be questionable. It can be

[3]The critical Mach number for the swept wing, based on simple-sweep concepts, is approximately 0.87.

noted from figure 7(c), however, that the various body modifications had little effect on the pitching-moment coefficients except near zero lift where, particularly at transonic speeds, the modifications reduced the variation of dC_m/dC_L with C_L.

Pressure Studies

Pressure distributions were measured chordwise near the wing mid-semispan and along one side of the bodies at the wing-body junction.

Wing pressures.- A comparison of wing pressure distributions at several Mach numbers, measured near the wing mid-semispan, for the various models at zero angle of attack is presented in figure 10. The various body modifications resulted in large changes in the pressure distributions on the wing, particularly on the after part at the transonic Mach numbers. The more favorable pressure distributions resulting from the body modifications are evident, especially for the area-rule modification at 0.94 Mach number and for the Kuchemann modification at a Mach number of 1.00.

Pressures at wing-body junction.- A comparison of pressure distributions at the wing-body junctions for the various models at zero angle of attack is presented in figure 11. The pressure distribution near the wing root of the basic model is considered to be unfavorable since the point of minimum pressure is far aft of the mid-chord station with the probable result that the isobars of the swept wing have little or no sweep near the wing root. The loss of sweep for the isobars is thought to be undesirable at high subsonic speeds since critical conditions seem to depend not on the total velocities, but on the velocity components in the direction of the pressure gradients (that is, normal to the isobars).

The slight body modification of model 1 did much to correct the unfavorable distribution. The area-rule and Kuchemann modifications gave somewhat similar pressure distributions at the root chord throughout the speed range. However, the pressures for the Kuchemann modification indicate that a region of high velocities appeared at high subsonic Mach numbers just downstream of the root trailing edge. This region of high induced velocities was the result of a sudden increase in body radius due to the abruptness with which the Kuchemann modification was terminated near the trailing edge. It seems from this investigation that Kuchemann's method should be extended so as to take into account disturbances forward and aft of the wing root.

GENERAL DISCUSSION

It should be emphasized that the area-rule and Kuchemann modifications to the basic body shape were based on entirely different concepts. The area rule (design Mach number 1.00) was applied in an attempt to minimize the formation of wave drag; the Kuchemann procedure (design Mach number 0.87) was applied in an attempt to obtain the same flow near the root of the wing as that for the infinite yawed wing in order to realize the full benefit of sweep and consequently to obtain the highest possible drag-divergence Mach number.

The change in body shape for the area-rule model was considerable because of the large thickness-to-chord ratio of the wing, and the indentation occurred along a major portion of the body length due to the sweepback of the wing. The Kuchemann modification altered the basic body shape only in the vicinity of the junction, the modification terminating rather abruptly at the junction trailing edge.

The experimental data have shown that both the Kuchemann and the area-rule modifications resulted in considerably improved aerodynamic characteristics, not only at the respective design Mach numbers but also throughout the transonic speed range. The zero-lift drag results (fig. 8(a)) were somewhat surprising in that the area-rule model had the least drag at high subsonic Mach numbers while the Kuchemann model had the least drag at supersonic Mach numbers — a result contrary to what might be expected from the bases on which these modifications were designed. Although it is realized that insufficient pressure data were obtained to assess accurately the effects of the two body modifications, some conclusions can be made from the limited pressure data presented in figures 10 and 11.

To begin with, it is interesting to note the probable location of the shock near the wing mid-semispan as indicated by the pressure data in figure 10. At Mach numbers of 0.87, 0.90, and 0.94, for the Kuchemann model the shock appeared to be behind the location for the area-rule model but at Mach numbers of 1.00 and 1.06 the respective locations seemed to be reversed. The wing pressure distributions shown in figure 10 provide some insight to the probable reasons why the area-rule model had the least drag at high subsonic speeds while the Kuchemann model had the least drag at supersonic speeds.

At the wing-body junction the pressure distributions were quite similar for the two models (fig. 11). However, a region of high velocities appeared on the body downstream of the junction for the Kuchemann model. Judging from the pressure distributions, this region terminated in a shock wave at Mach numbers of 0.90 and 0.94.

The considerably higher lift-curve slopes obtained by the Kuchemann model at transonic speeds (fig. 9) are believed to be due largely to the annular bump on the body mentioned above since an examination of wing pressure distributions at small angles of attack (not presented in this report) showed that the Kuchemann model had considerably higher loading near the junction trailing edge due primarily to more positive pressures on the wing lower surface.

CONCLUDING REMARKS

These tests show that important improvements in the aerodynamic characteristics at transonic speeds of a wing-body combination employing a thick swept wing of large aspect ratio can be obtained by modifications to the body shape.

In these experiments, the Kuchemann modification resulted in superior aerodynamic characteristics except with regard to zero-lift drag at high subsonic Mach numbers where the area-rule modification gave superior results. However, little difference between the two models was observed at 0.3 lift coefficient.

A greater reduction of the zero-lift drag at high subsonic Mach numbers than that for the model designed by the Kuchemann method is believed possible if more careful attention is given to the termination of the body modification near the trailing edge of the wing so as to avoid large body-induced velocities just downstream of the wing-body junction. However, a more gradual downstream termination of the Kuchemann modification might eliminate part of the drag reduction at the supersonic Mach numbers.

Ames Aeronautical Laboratory
National Advisory Committee for Aeronautics
Moffett Field, Calif., Feb. 21, 1955

REFERENCES

1. Jones, Robert T.: Subsonic Flow over Thin Oblique Airfoils at Zero Lift. NACA Rep. 902, 1948. (Supersedes NACA TN 1340)

2. Neumark, Stefan: Velocity Distribution on Straight and Sweptback Wings of Small Thickness and Infinite Aspect Ratio at Zero Incidence. R.A.E. Rep. No. Aero. 2200, British, May 1947.

3. Watkins, Charles E.: The Streamline Pattern in the Vicinity of an Oblique Airfoil. NACA TN 1231, 1947.

4. Boddy, Lee E.: Investigation at High Subsonic Speeds of Methods of Alleviating the Adverse Interference at the Root of a Swept-Back Wing. NACA RM A50E26, 1950.

5. Pepper, William B., Jr.: The Effect on Zero-Lift Drag of an Indented Fuselage or a Thickened Wing-Root Modification to a 45° Swept-Back Wing-Body Configuration as Determined by Flight Test at Transonic Speeds. NACA RM L51F15, 1951.

6. Kuchemann, Dietrich: Design of Wing Junction, Fuselage and Nacelles to Obtain the Full Benefit of Sweptback Wings at High Mach Number. R.A.E. Rep. No. Aero. 2219, British, Oct. 1947.

7. Weber, J.: Design of Wing Junction, Fuselage and Nacelles to Obtain the Full Benefit of Sweptback Wings at High Mach Number. Addendum: Additional Tables of Coefficients. R.A.E. Rep. No. Aero. 2219(a), British, May 1949.

8. McDevitt, John B., and Haire, William M.: Investigation at High Subsonic Speeds of a Body-Contouring Method for Alleviating the Adverse Interference at the Root of a Sweptback Wing. NACA RM A54A22, 1954.

9. Hartley, D. E.: Investigation at High Subsonic Speeds of Wing-Fuselage Intersection Shapes for Sweptback Wings. Part I. Force Measurements on Some Initial Designs. R.A.E. Rep. No. Aero. 2464, British, May 1952.

10. Hartley, D. E.: Investigation at High Subsonic Speeds of Wing-Fuselage Intersection Shapes for Sweptback Wings. Part II. Pressure Measurements on Some Initial Designs. R.A.E. Rep. No. Aero. 2503, British, Dec. 1953.

11. Whitcomb, Richard T.: A Study of the Zero-Lift Drag-Rise Characteristics of Wing-Body Combinations Near the Speed of Sound. NACA RM L52H08, 1952.

12. Howell, Robert R., and Braslow, Albert L.: An Experimental Study of a Method of Designing the Sweptback Wing Fuselage Juncture for Reducing the Drag at Transonic Speeds. NACA RM L54L31a, 1954.

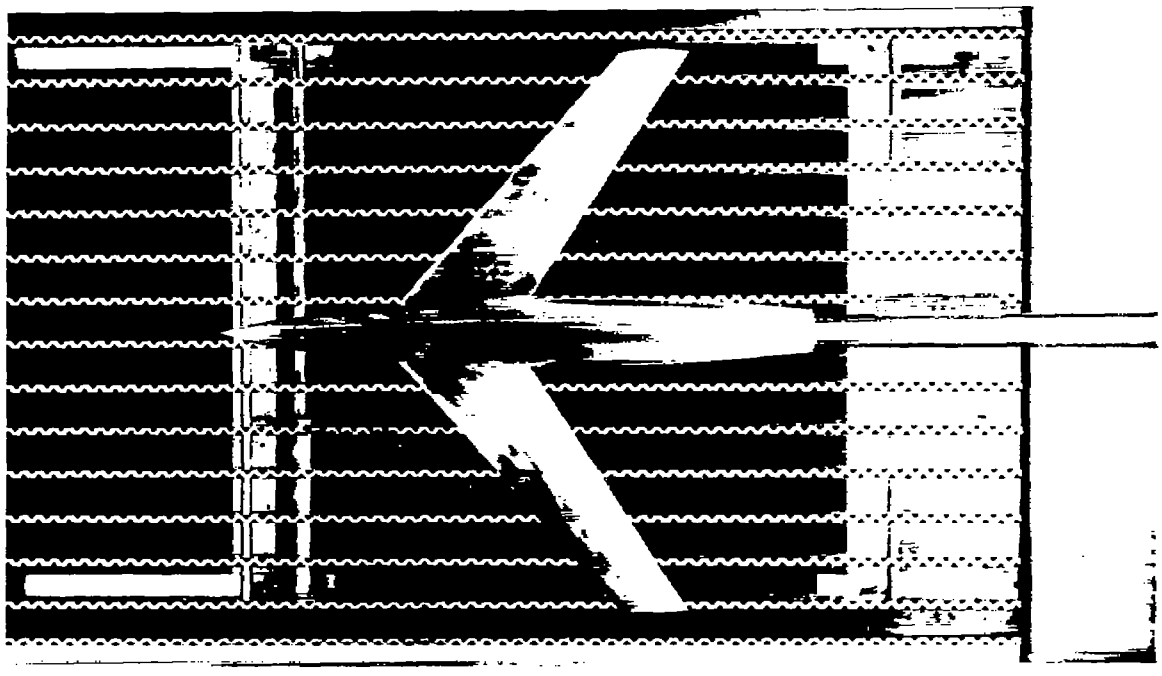

A-19246.1

(a) Basic model.

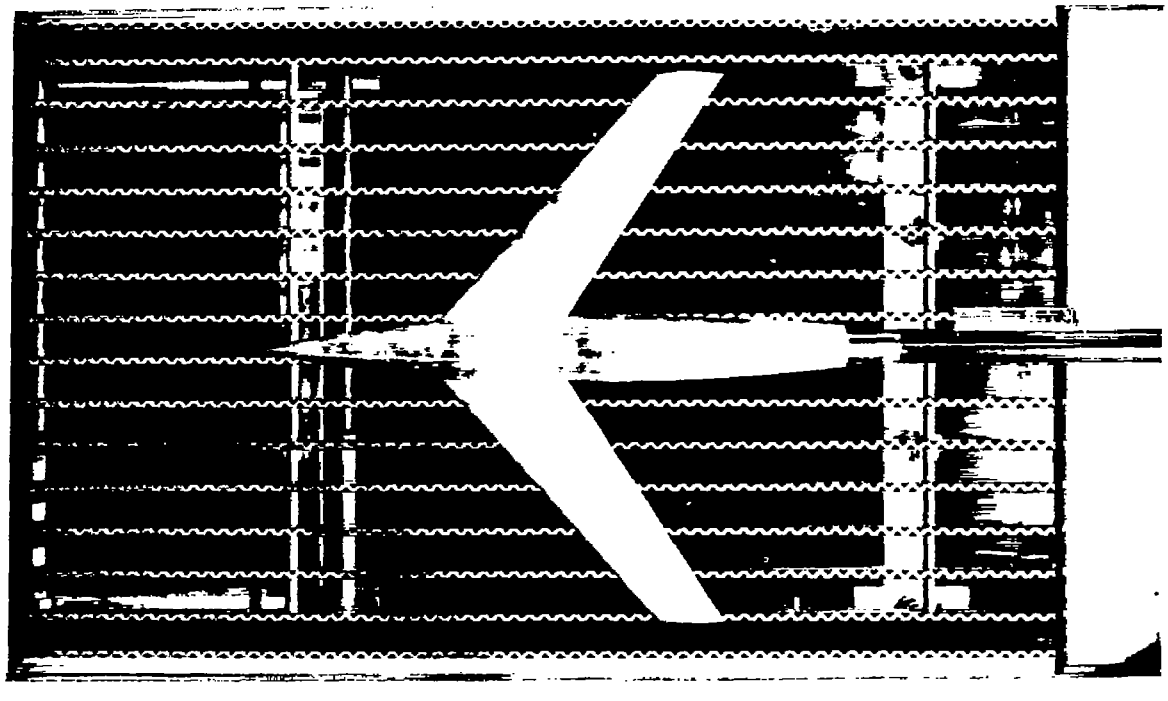

A-19236.1

(b) Model 1.

Figure 1.- Photographs of the models.

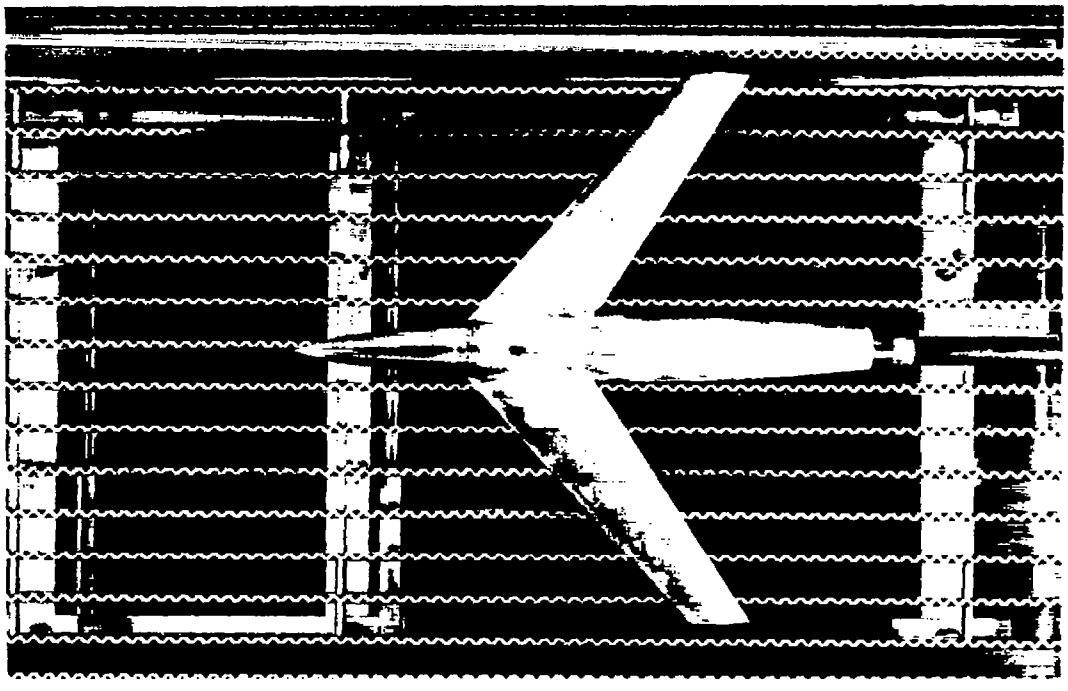

(c) Model 2 (Kuchemann). A-19632.1

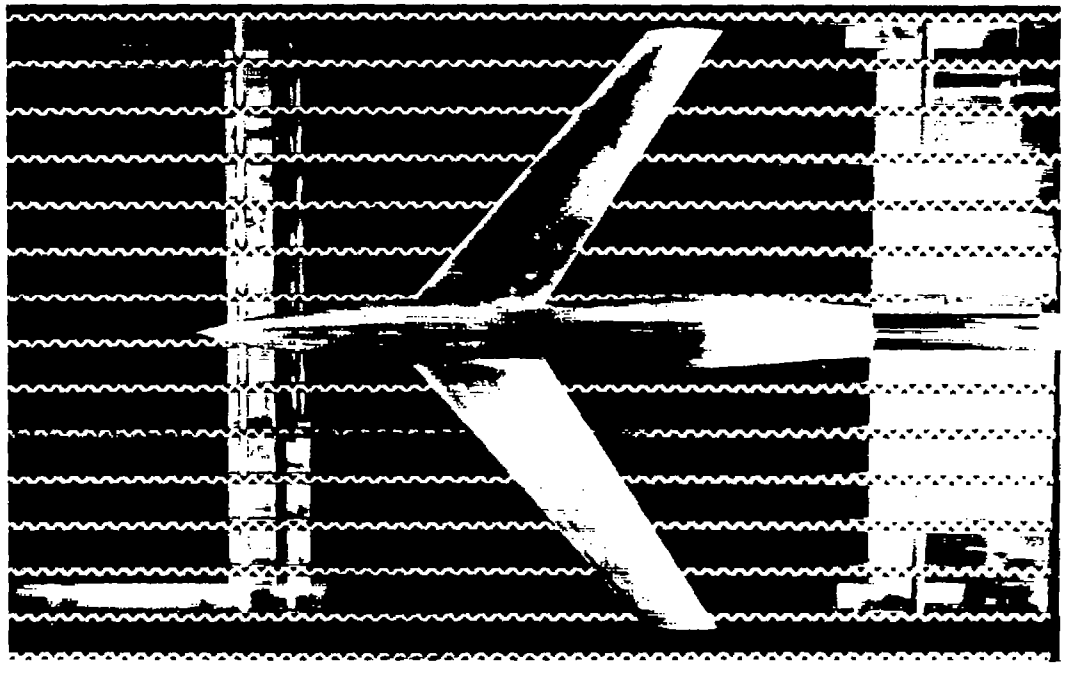

(d) Model 3 (area rule). A-19269.1

Figure 1.- Concluded.

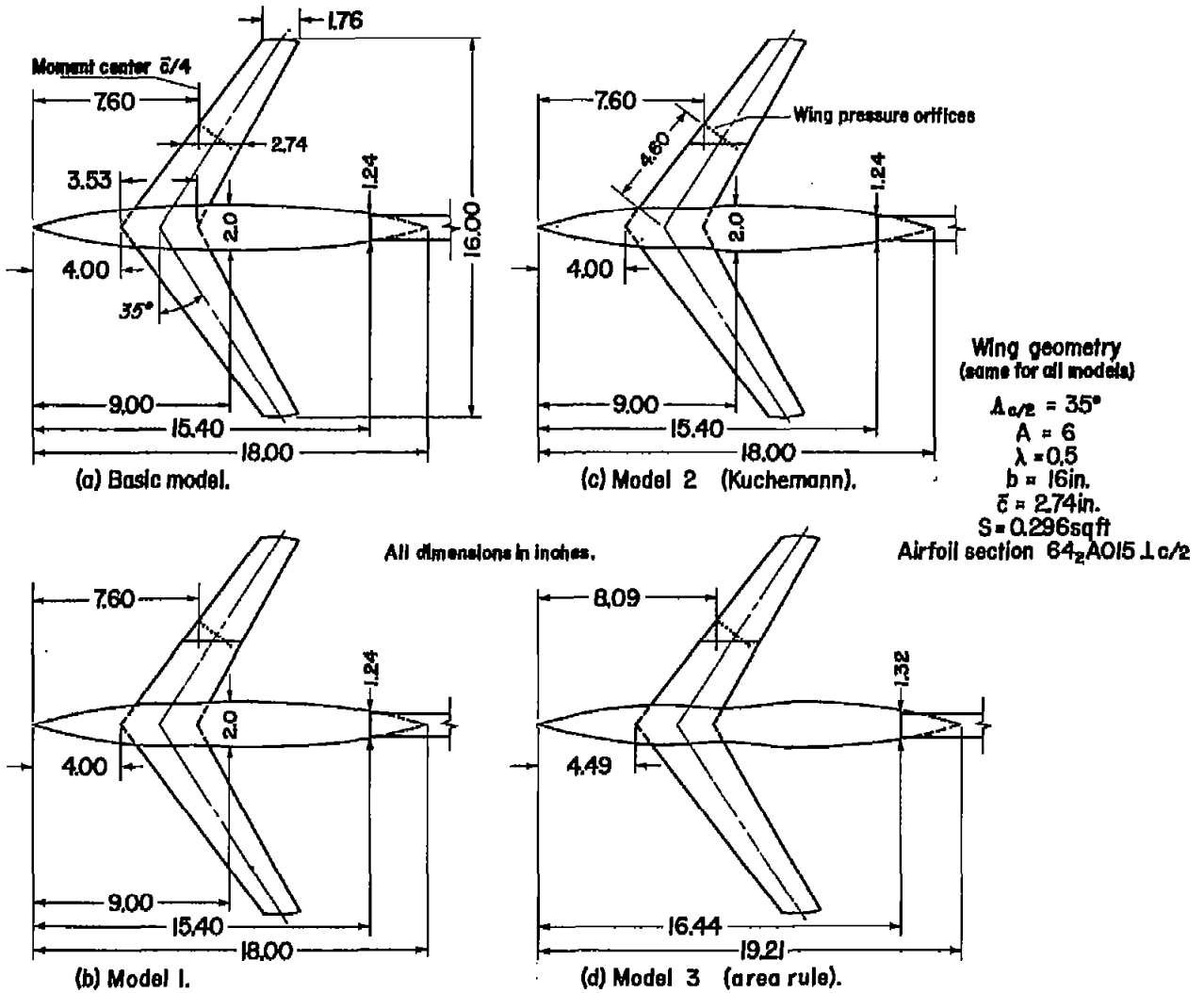

Figure 2.- Plan forms of the models.

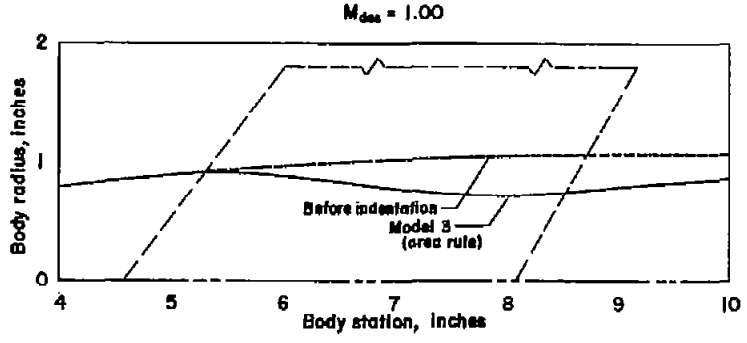

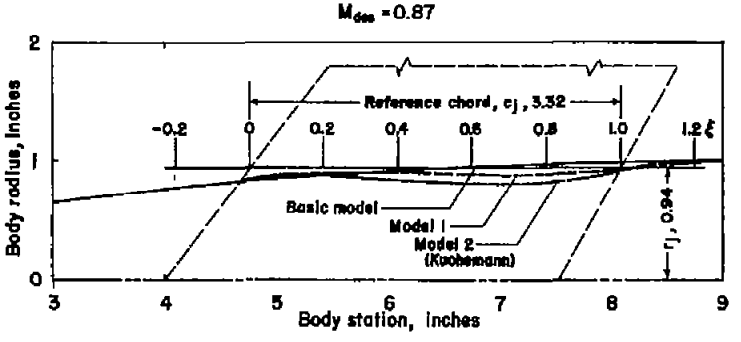

Body station, in.	Body radius, in.	
	Before indentation	Model 3 (area rule)
0	0	0
1.00	.317	.317
2.00	.508	.508
3.00	.660	.660
4.00	.782	.782
5.00	.877	.877
5.50	.917	.900
6.00	.952	.875
6.50	.982	.827
7.00	1.008	.772
7.50	1.028	.728
8.00	1.045	.712
8.50	1.057	.735

Body station, in.	Body radius, in.	
	Before indentation	Model 3 (area rule)
9.00	1.064	0.783
9.50	1.067	.823
10.00	1.066	.855
10.50	1.062	.877
11.00	1.051	.893
11.50	1.036	.934
12.00	1.017	.975
12.50	.993	.988
13.00	.967	.967
14.00	.893	.893
15.00	.803	.803
16.00	.704	.704
16.44	.660	.660

Body station, in.	ξ	Basic body radius, in.	Body radius, in.	
			Model 1	Model 2
4.096	-0.2	0.768	0.768	0.768
4.428	-.1	.800	.804	.800
4.760	0	.830	.846	.880
5.092	.1	.855	.878	.882
5.424	.2	.879	.898	.873
5.756	.3	.902	.907	.856
6.088	.4	.928	.902	.838
6.420	.5	.938	.896	.820
6.752	.6	.953	.890	.811
7.084	.7	.964	.888	.805
7.416	.8	.975	.890	.819
7.748	.9	.983	.903	.851
8.080	1.0	.990	.965	.921
8.412	1.1	.994	.956	.978
8.744	1.2	.998	.977	.995

Figure 3.- Body contour details.

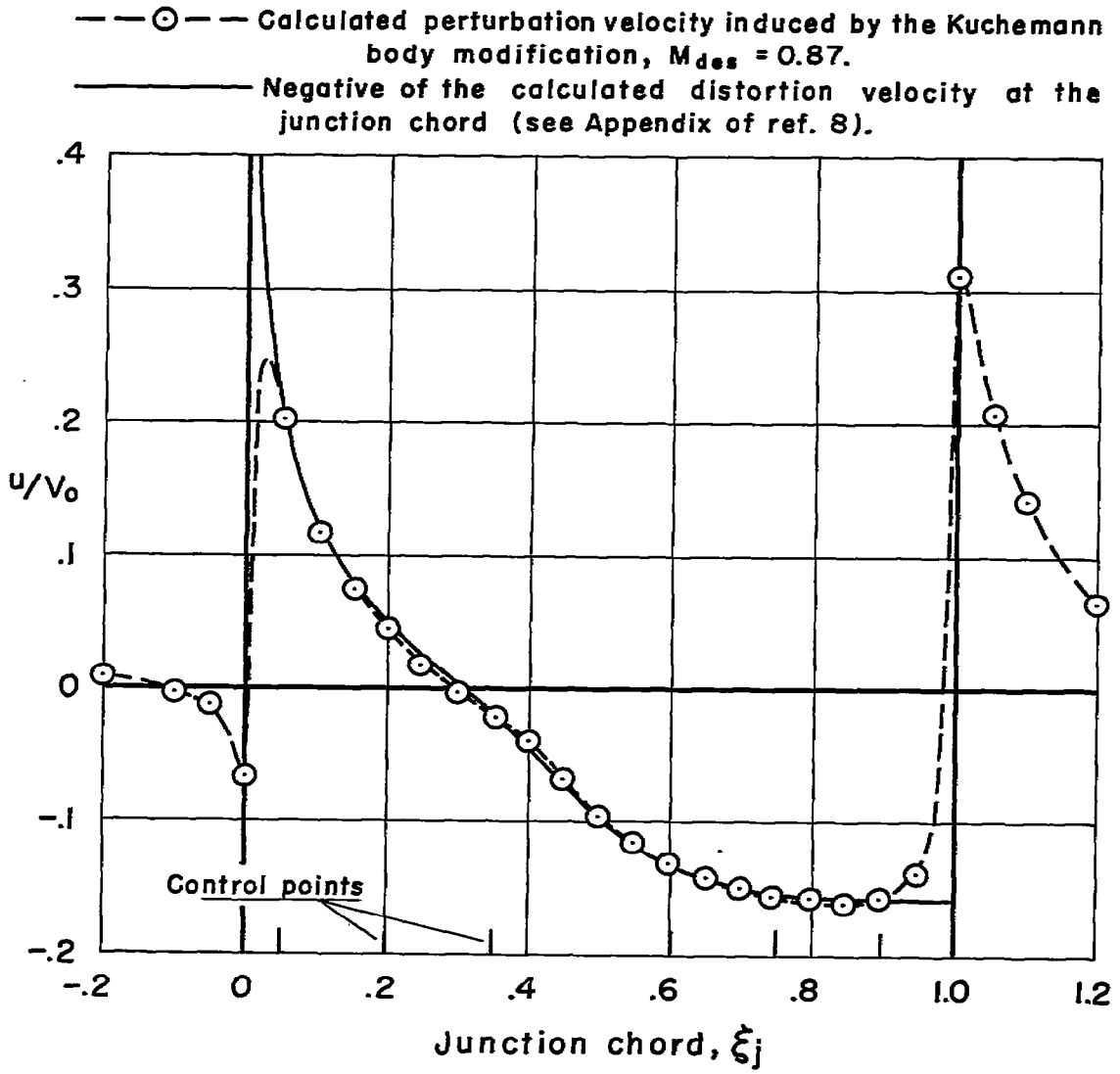

Figure 4.- Comparison of velocities induced by the Kuchemann body modification with the negative of the distortion velocities at the junction chord.

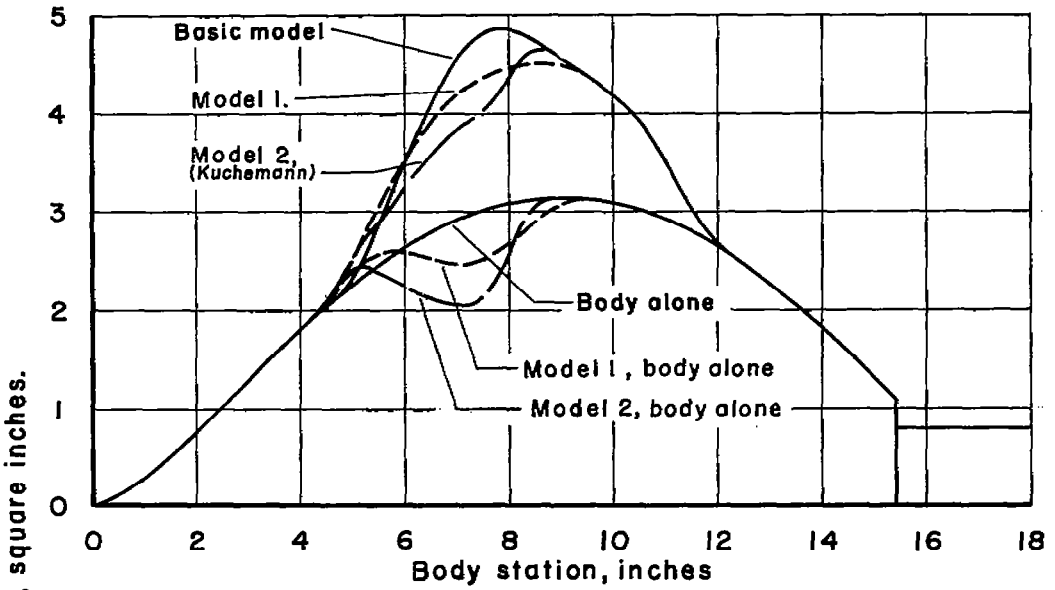

(a) Models 1 and 2 (Kuchemann).

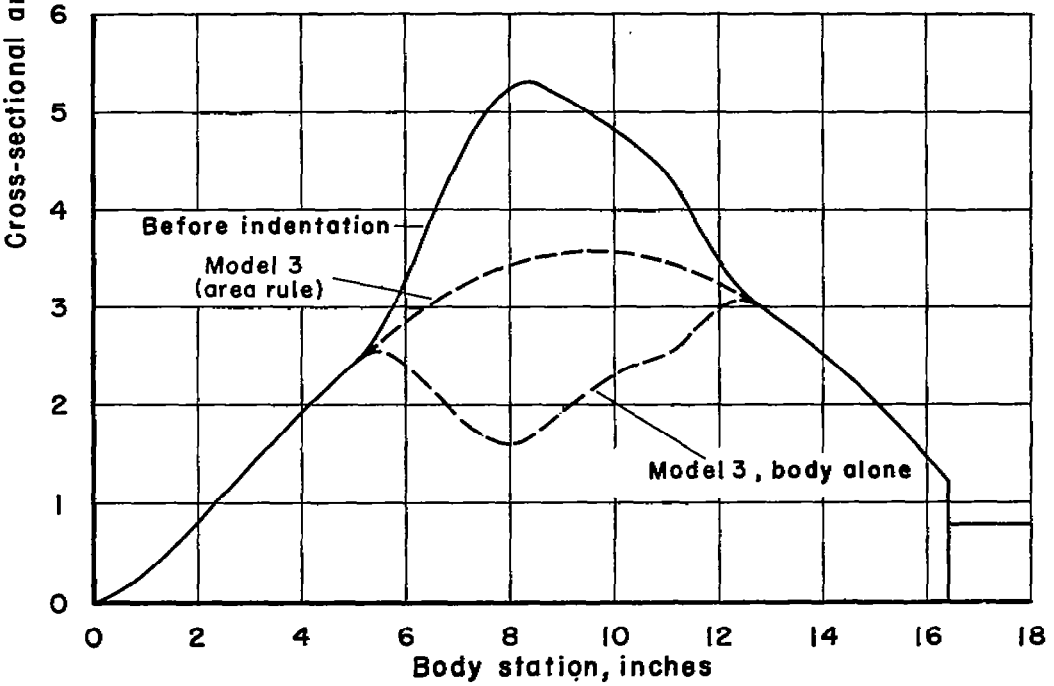

(b) Model 3 (area rule).

Figure 5.- Cross-sectional area distributions of the models.

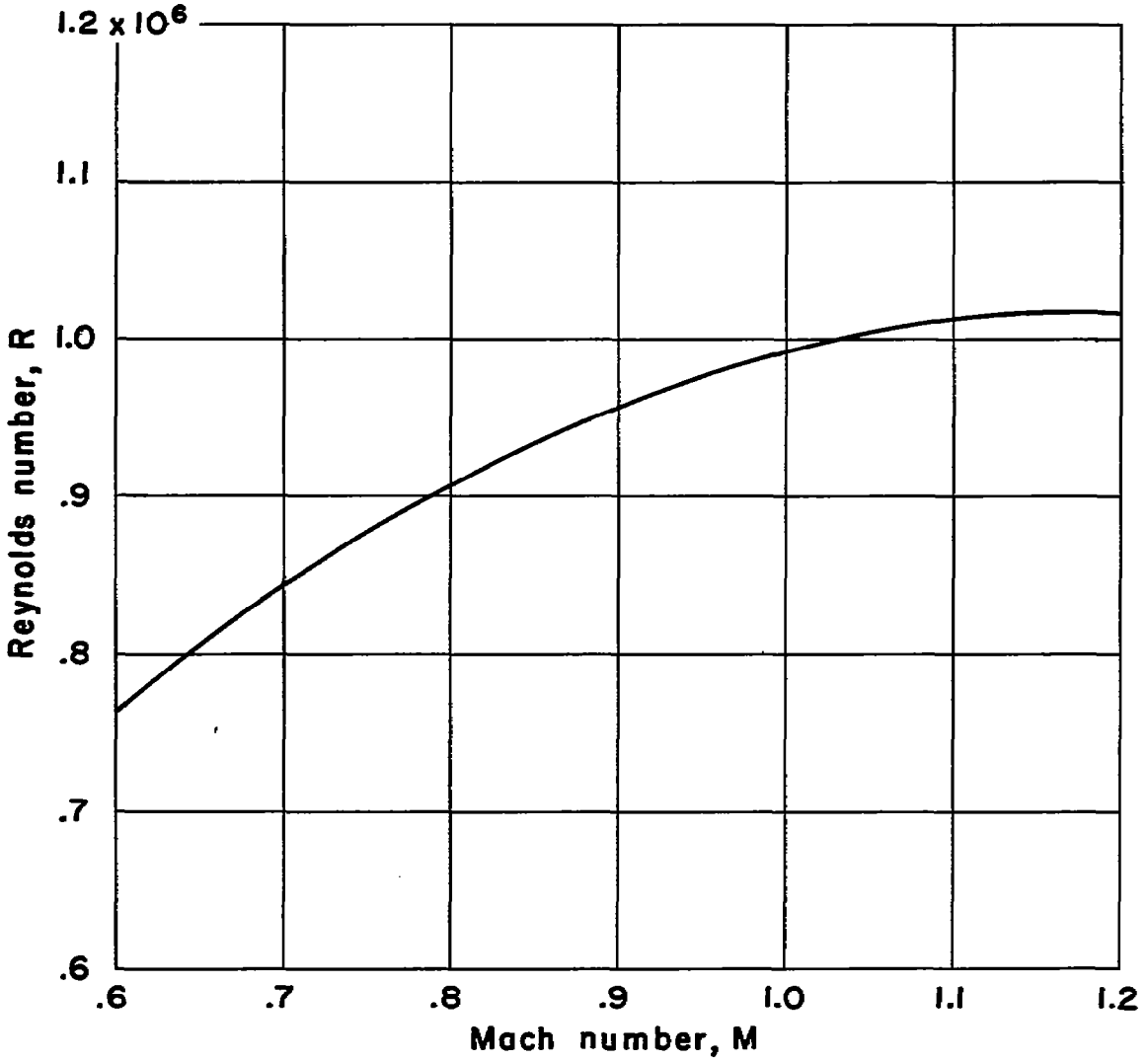

Figure 6.- Variation of Reynolds number with Mach number.

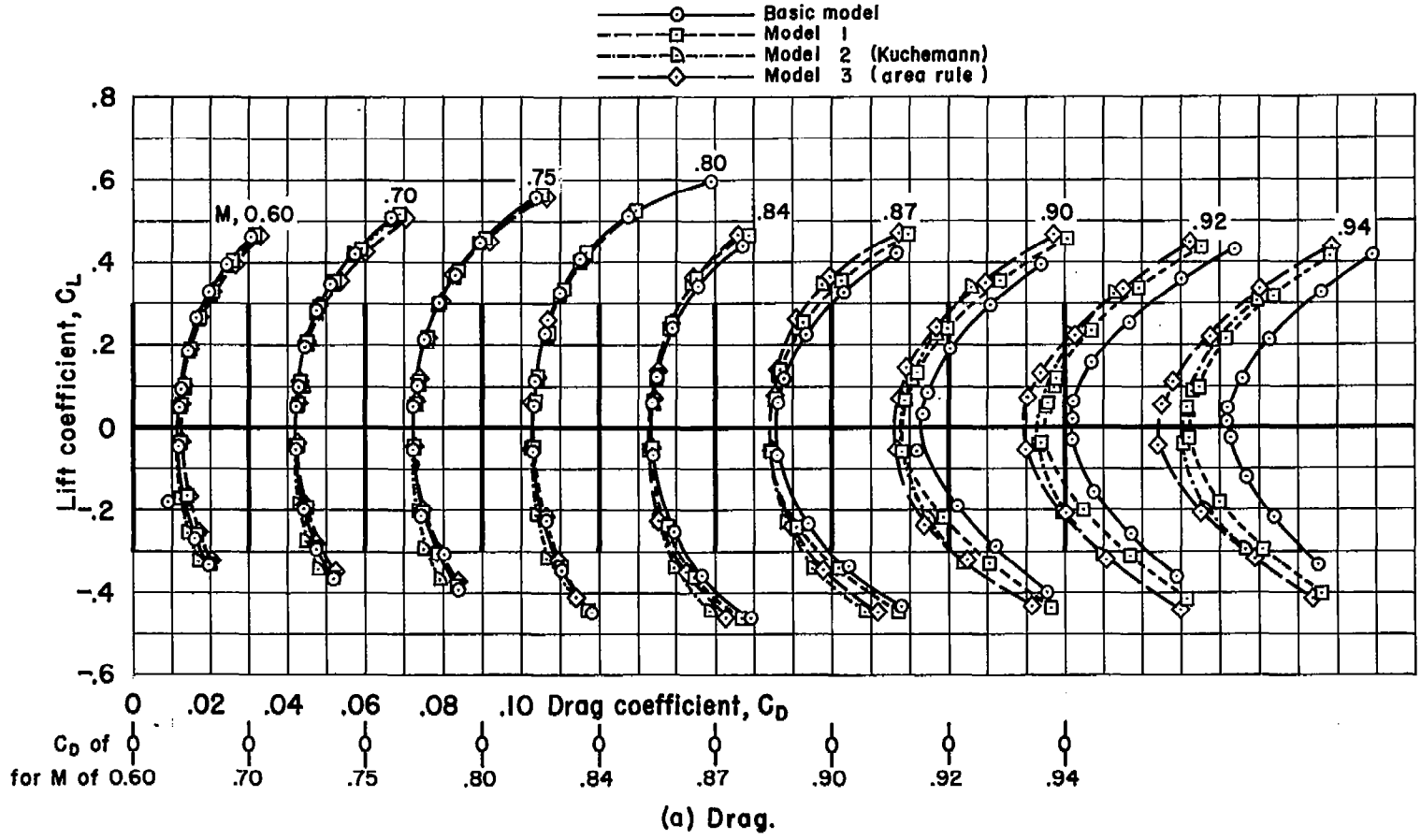

(a) Drag.

Figure 7.- Drag, lift, and pitching-moment characteristics of the models.

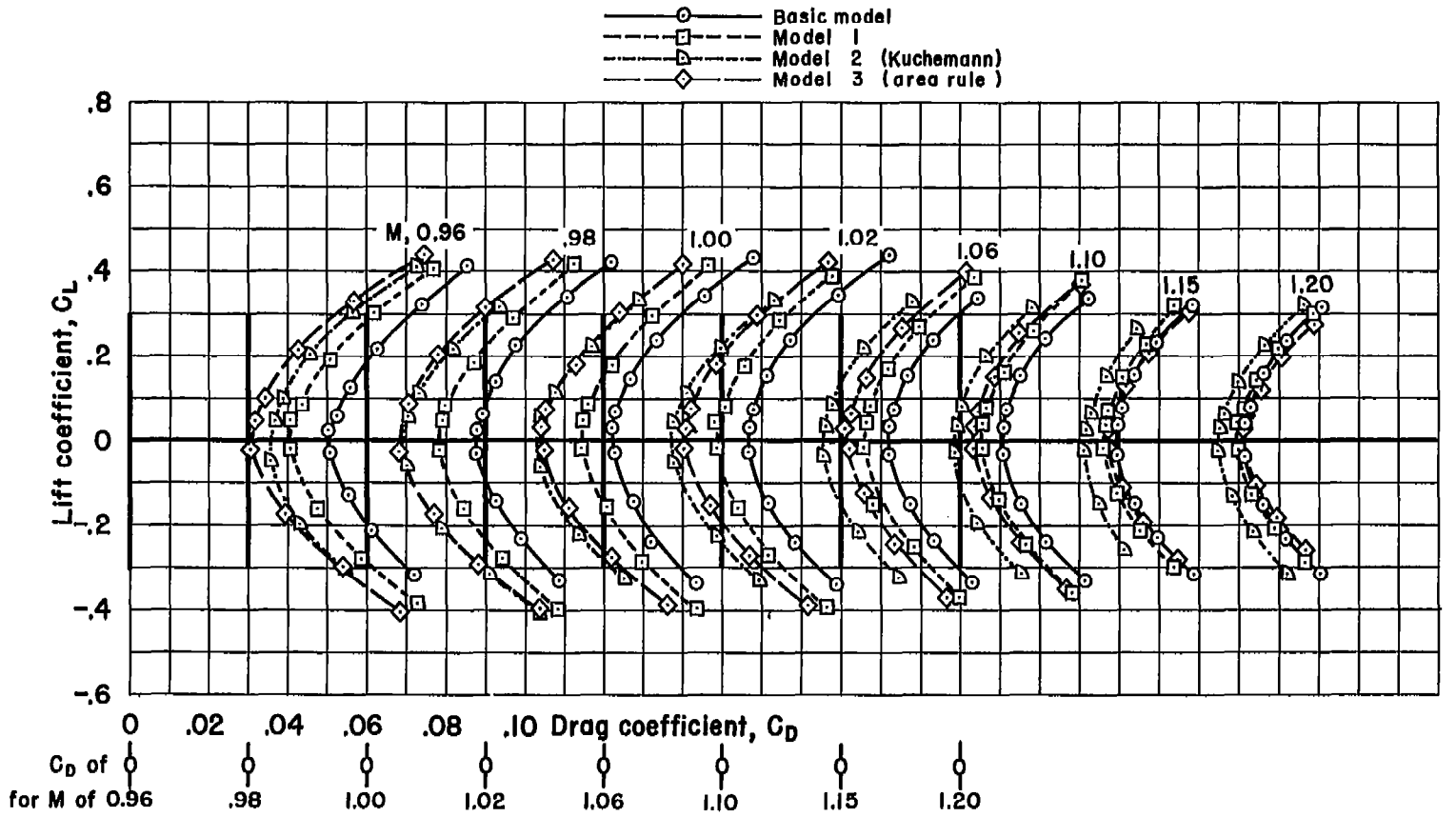

(a) Concluded.

Figure 7.- Continued.

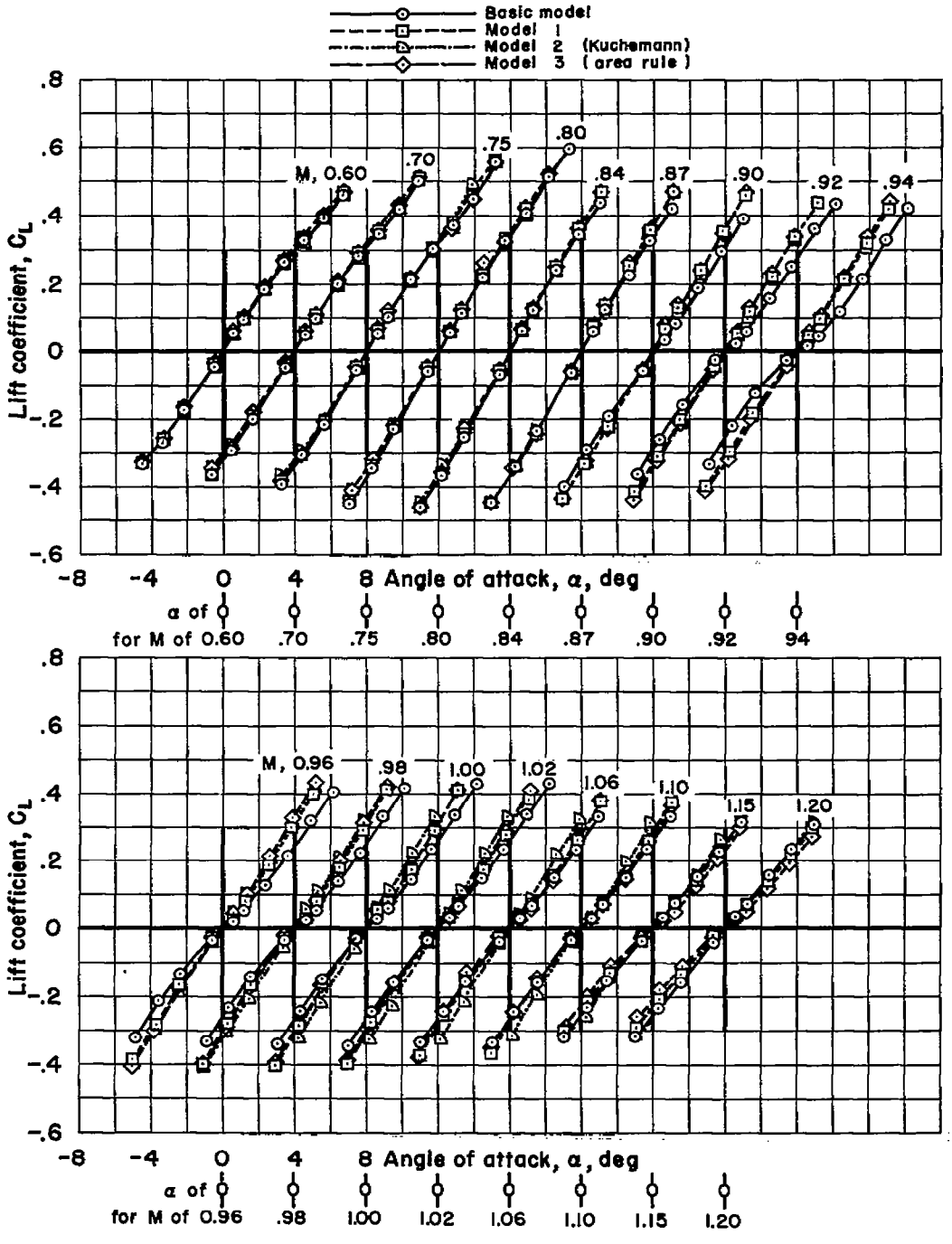

(b) Lift.

Figure 7.- Continued.

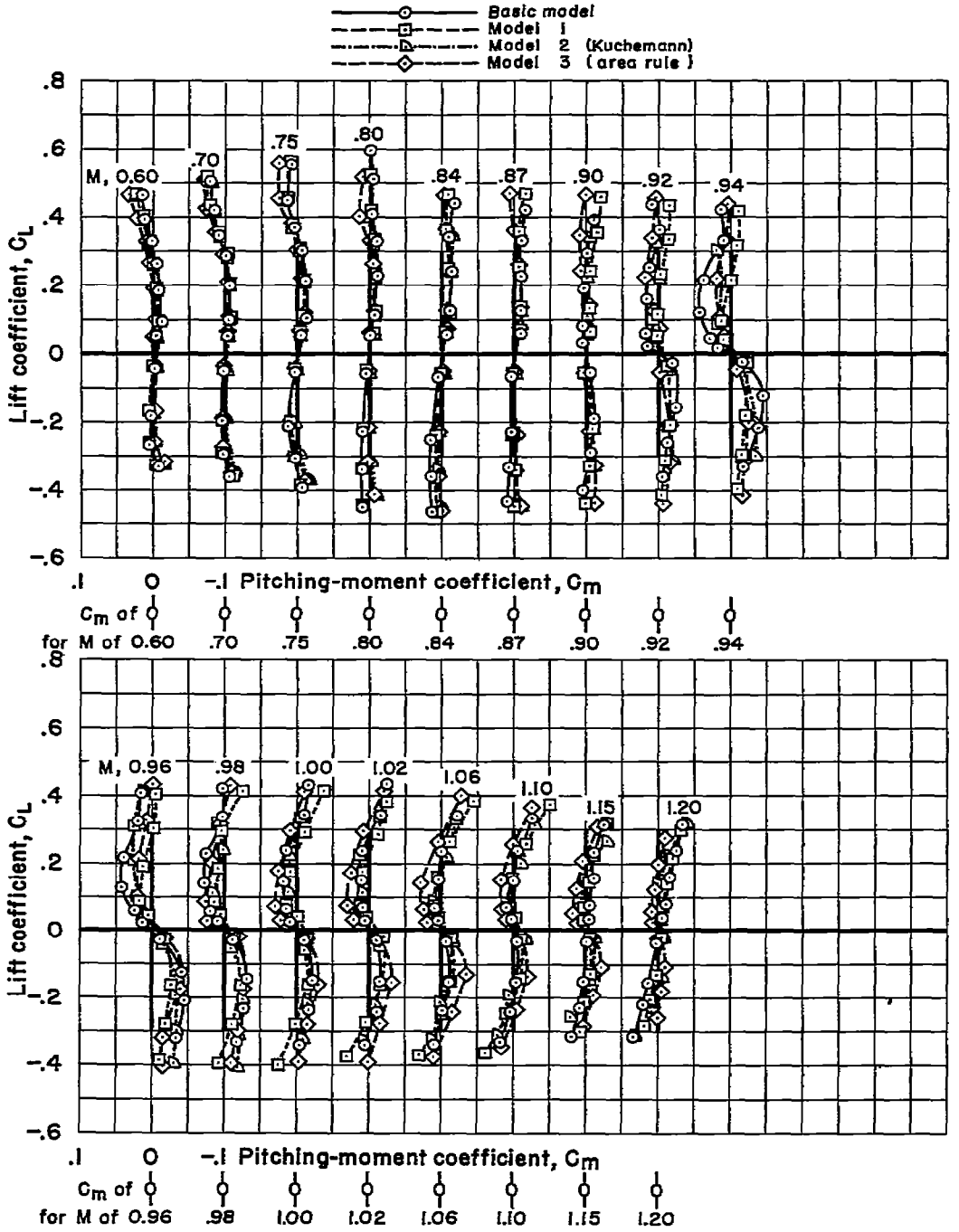

(c) Moment.

Figure 7.- Concluded.

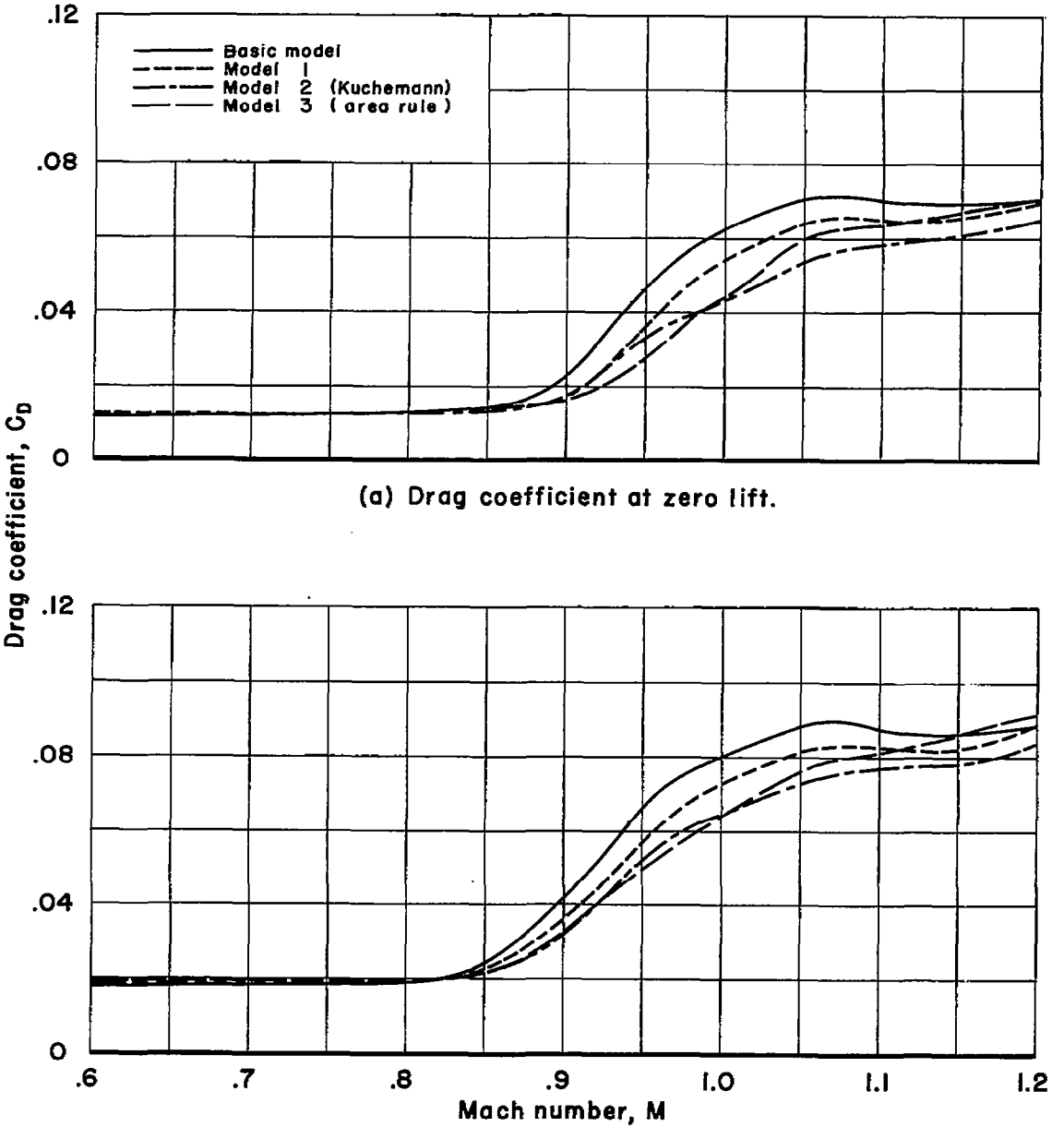

Figure 8.- Variation of drag coefficient with Mach number.

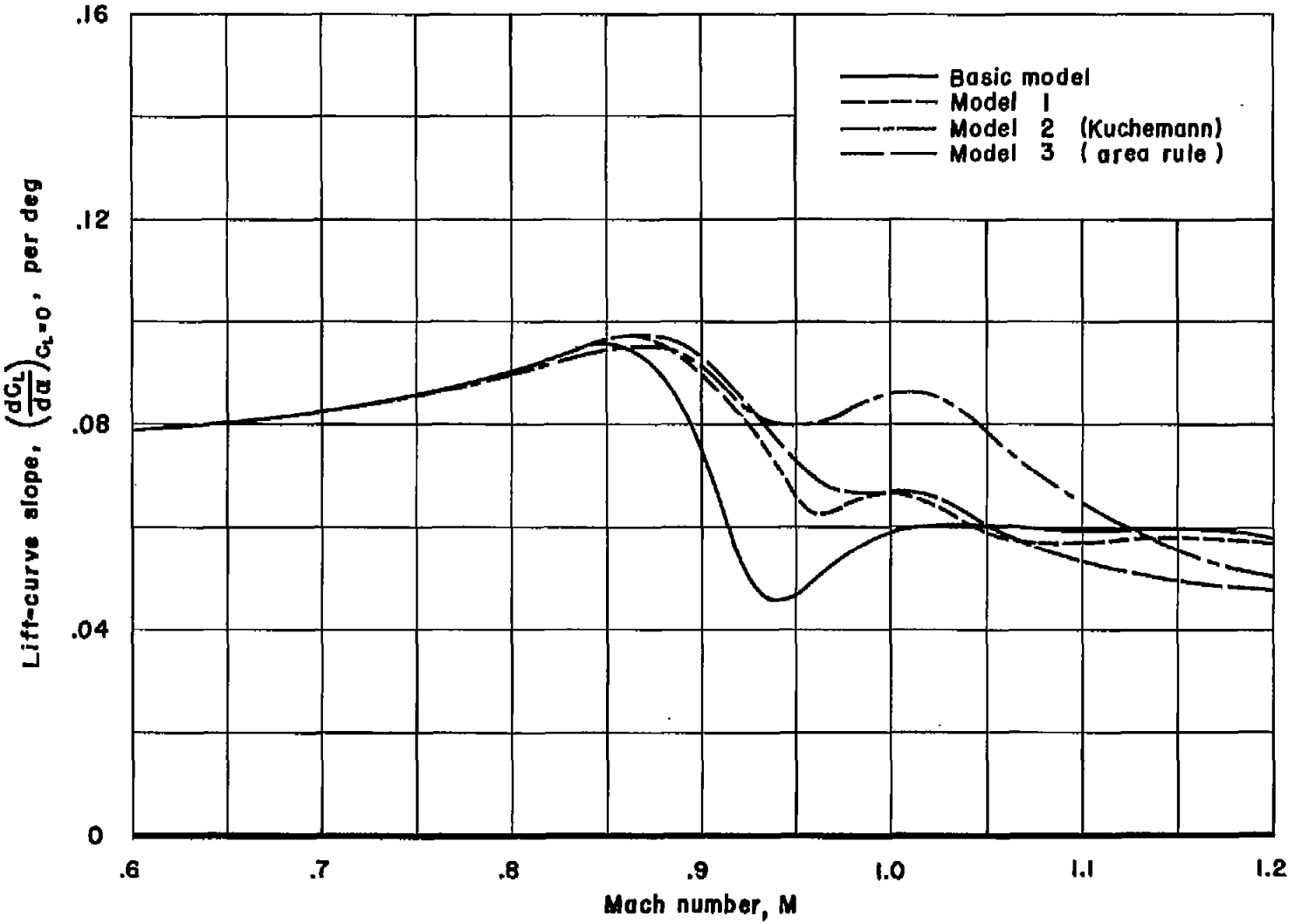

Figure 9.- Variation of lift-curve slope with Mach number.

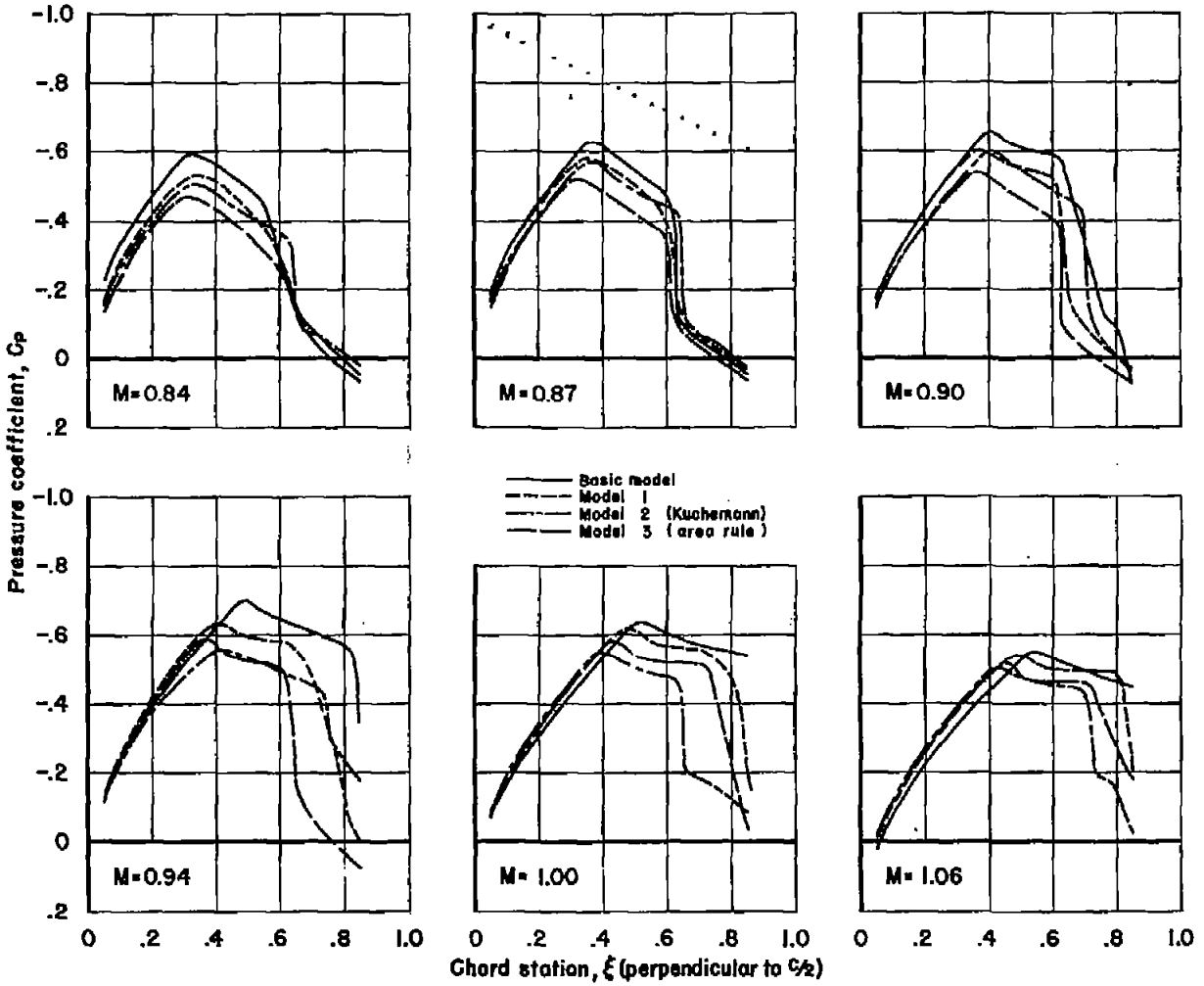

Figure 10.- Comparison of pressures at the wing mid-semispan for the various models at zero angle of attack.

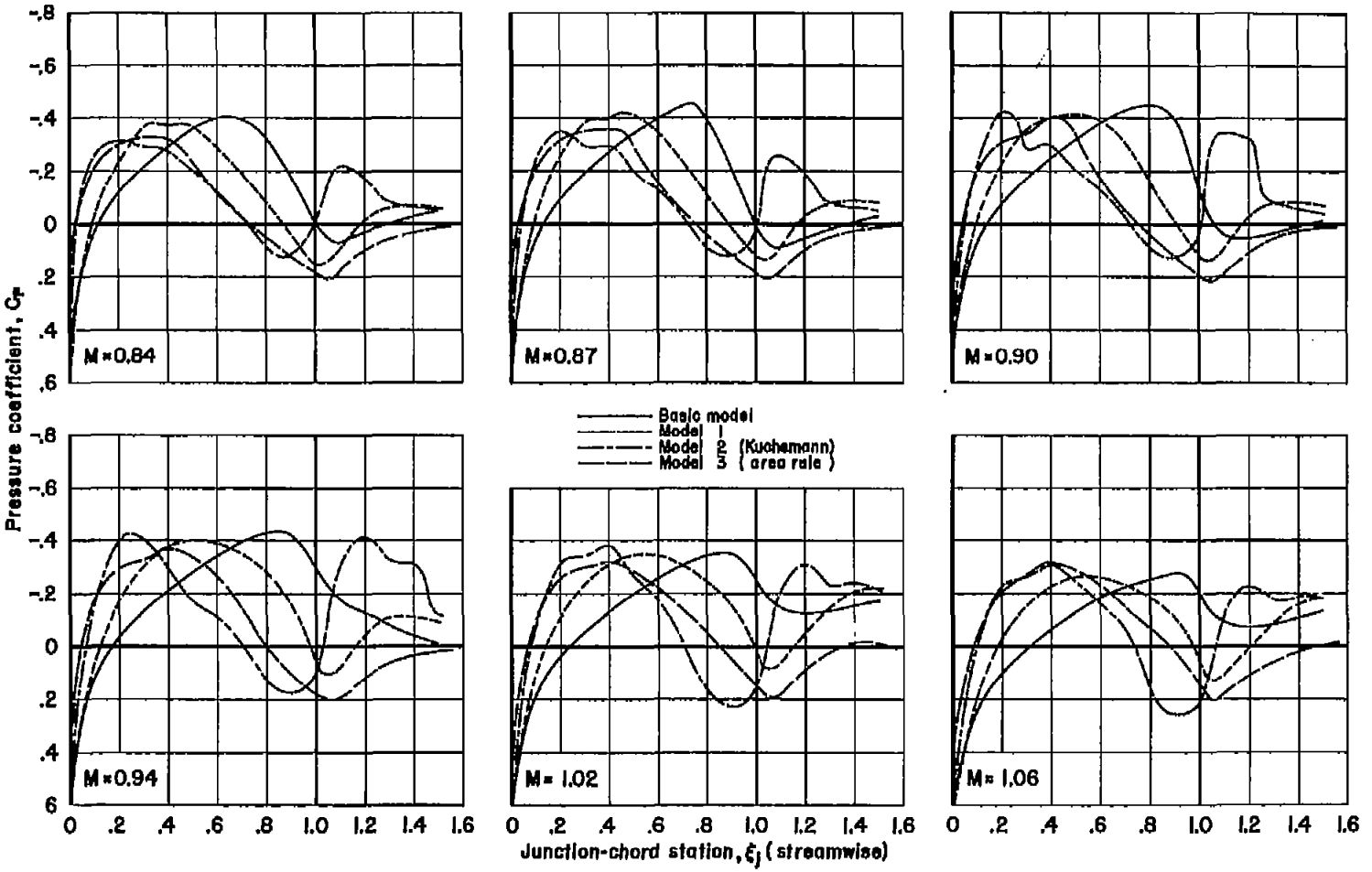

Figure 11.- Comparison of pressures at the wing-body junction for the various models at zero angle of attack.